Smart Structures and Systems, *Vol. 17, No. 3 (2016) 471-489*
DOI: http://dx.doi.org/10.12989/sss.2016.17.3.471

Mode identifiability of a cable-stayed bridge based on a Bayesian method

Feng-Liang Zhang[1a], Yi-Qing Ni[2b] and Yan-Chun Ni[*1]

[1]*Research Institute of Structural Engineering and Disaster Reduction, Tongji University, Shanghai, China*
[2]*Department of Civil and Environmental Engineering, The Hong Kong Polytechnic University, Hung Hom, Kowloon, Hong Kong*

(Received July 1, 2015, Revised October 18, 2015, Accepted December 25, 2015)

Abstract. Modal identification based on ambient vibration data has attracted extensive attention in the past few decades. Since the excitation for ambient vibration tests is mainly from the environmental effects such as wind and traffic loading and no artificial excitation is applied, the signal to noise (s/n) ratio of the data acquired plays an important role in mode identifiability. Under ambient vibration conditions, certain modes may not be identifiable due to a low s/n ratio. This paper presents a study on the mode identifiability of an instrumented cable-stayed bridge with the use of acceleration response data measured by a long-term structural health monitoring system. A recently developed fast Bayesian FFT method is utilized to perform output-only modal identification. In addition to identifying the most probable values (MPVs) of modal parameters, the associated posterior uncertainties can be obtained by this method. Likewise, the power spectral density of modal force can be identified, and thus it is possible to obtain the modal s/n ratio. This provides an efficient way to investigate the mode identifiability. Three groups of data are utilized in this study: the first one is 10 data sets including six collected under normal wind conditions and four collected during typhoons; the second one is three data sets with wind speeds of about 7.5 m/s; and the third one is some blind data. The first two groups of data are used to perform ambient modal identification and help to estimate a critical value of the s/n ratio above which the deficient mode is identifiable, while the third group of data is used to perform verification. A couple of fundamental modes are identified, including the ones in the vertical and transverse directions respectively and coupled in both directions. The uncertainty and s/n ratio of the deficient mode are investigated and discussed. A critical value of the modal s/n ratio is suggested to evaluate the mode identifiability of the deficient mode. The work presented in this paper could provide a base for the vibration-based condition assessment in future.

Keywords: mode identifiability; cable-stayed bridge; ambient vibration; fast Bayesian FFT method; uncertainty

1. Introduction

Structural health monitoring (SHM) has attracted increasing attention in the past two decades with the purpose of monitoring structural performance and conducting condition assessment of

∗Corresponding author, Postdoctoral Fellow, E-mail: yanchunni@gmail.com
[a] Assistant Professor, E-mail: fengliangzhang@hotmail.com
[b] Professor, E-mail: ceyqni@polyu.edu.hk

http://www.techno-press.org/?journal=sss&subpage=8 ISSN: 1738-1584 (Print), 1738-1991 (Online)

objective structures (Brownjohn *et al*. 2005, Ko and Ni 2005, Li *et al*. 2006, Ni *et al*. 2011, Koo *et al*. 2013). Among a variety of structural response, acceleration plays an important role in deriving the baseline properties of a structure. In general, there are three ways to collect structural acceleration response, i.e., ambient, free and forced vibration tests (Au and Ni 2014). Ambient vibration tests have been widely practiced since they are more economical and convenient in comparison with the other two. For large-scale bridges, the SHM system is commonly designed to collect various structural responses including acceleration. A lot of research has been pursued on the analysis of acceleration response data acquired by SHM systems (Li *et al*. 2006, Bao *et al*. 2010, Cross *et al*. 2013, Ni *et al*. 2015b).

With the collected acceleration data, modal identification is usually the first step to identify the modal parameters (Brownjohn *et al*. 2010), which can be further used for model updating and vibration-based damage detection (Lam *et al.* 2014). Various methods have been proposed for extracting modal properties from acceleration response. Among them the frequency domain decomposition (Brincker *et al*. 2001) is a commonly used technique in the context of frequency domain, while the stochastic subspace identification (SSI) (Peeters and De Roeck 2001) is a popular one in the time domain. A fast Bayesian FFT method has recently been developed (Au 2011, Au 2012a, b, Au and Zhang 2012a, Zhang *et al*. 2015), which considers ambient modal identification as an inference problem where probability is used as a measure for the relative plausibility of outcomes. One important merit of this method is that it can calculate the posterior uncertainty of the modal parameters analytically, making it possible to evaluate the accuracy and reliability of the identified modal parameters. This method has been applied for modal analysis of different kinds of structures (Au and Zhang 2012, Au *et al*. 2012a, b, Au *et al.* 2013, Zhang *et al*. 2016, Ni *et al*. 2016).

In ambient modal identification, mode identifiability is a key issue worth investigating (Ni *et al*. 2015a). Signal to noise (s/n) ratio is an important factor affecting the identifiability. If the s/n ratio for a specific mode is too low, the identification of this mode will be of high uncertainty, and even being unidentifiable. The measurement noise usually stems from the deployed sensors, signal cables, and data acquisition systems. One efficient way of improving the s/n ratio is to lower the noise corruption. On the other hand, increasing the excitation intensity is equally efficient. For bridge structures, the excitation level during a typhoon or earthquake is usually much higher than ambient vibration excitations. As a result, some deficient modes that cannot be identified under normal wind conditions may become identifiable during typhoons. In this study, a benchmark problem on the mode identifiability of a cable-stayed bridge is addressed by the fast Bayesian FFT method. Three groups of data acquired from the bridge are used in the study: the first group includes ten data sets with six under normal wind conditions and four under typhoon conditions; the second group includes three data sets with wind speeds of about 7.5 m/s; and the third group is blind data with unknown wind condition, which serves to check the conclusions drawn from the analysis on the first two groups of data. The posterior uncertainties of the identified modal parameters are evaluated by the fast Bayesian FFT method, and the modal s/n ratio is obtained by the identified modal frequency, damping ratio, power spectral density (PSD) of modal force and PSD of prediction error to examine the mode identifiability of the deficient mode. A critical value of the s/n ratio is suggested to judge whether or not a specific mode is identifiable.

2. Ting Kau Bridge

The benchmark study is based on the field monitoring data from the cable-stayed Ting Kau Bridge, which is 1170 m long in total with two main spans of 448 m and 475 m, respectively. A long-term structural health monitoring system has been deployed on the bridge to monitor the structural performance under in-service conditions. Sensors permanently instrumented on the bridge include accelerometers, anemometers, displacement transducers, temperature sensors, strain gauges, GPS and a weigh-in-motion sensing system. Accelerometers were installed at different locations of the bridge including the deck of the two main spans and two side spans, the longitudinal stabilizing cables, the top of the three towers, and the base of the central tower. In the present study, only the acceleration responses at the bridge deck are addressed. As shown in Figure 1, a total of 24 uniaxial accelerometers have been deployed on the bridge deck, where 16 located at the east and west sides of the longitudinal steel girders (Locations 1, 3, 4, 6, 7, 9, 10, 12, 13, 15, 16, 18, 19, 21, 22 and 24) are along the vertical direction, while 8 located at the central crossgirder (Locations 2, 5, 8, 11, 14, 17, 20 and 23) are in the transverse direction. The sampling rate was set as 25.6 Hz. The wind data measured from anemometers situated at the bridge deck and tower top are also utilized in the analysis. The sampling rate of the wind data was set as 2.56 Hz.

As mentioned before, three groups of data are available for this study. The first group of 10 data sets is summarized in Table 1 and the second group of three data sets with wind speeds of about 7.5 m/s is shown in Table 2. The third group consists of six blind data sets without knowledge about the wind condition. The data length for each set is 1 hour. From Table 1, it is seen that the wind speeds under typhoons are much higher than those under normal wind conditions. The first two groups of data serve to investigate the mode identifiability of the bridge while the third one is utilized to verify the conclusions drawn from the analysis on the first two groups of data.

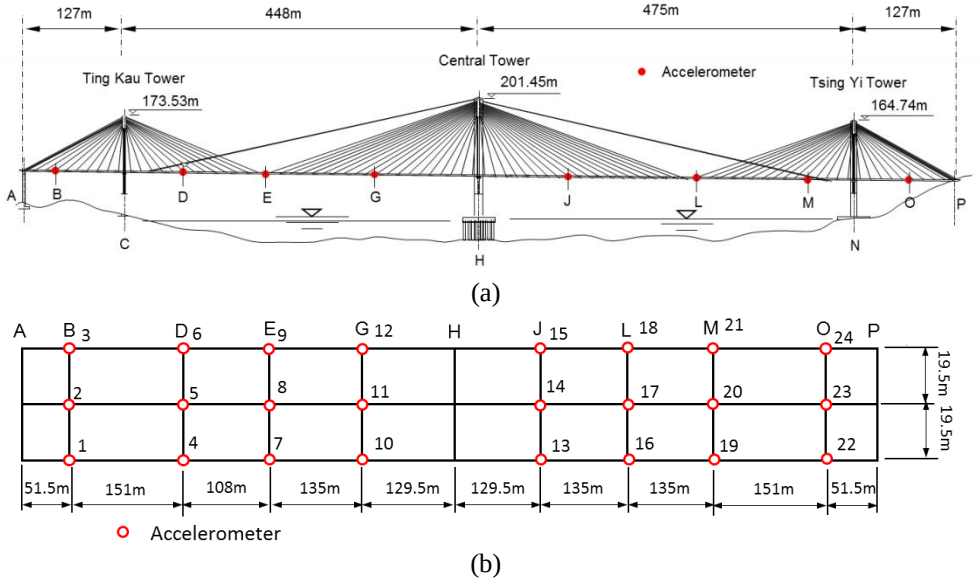

Fig. 1 (a) Layout of accelerometers on bridge deck and (b) Plan view of sensor configuration (Ni *et al.* 2015a)

Table 1 Wind information for data in Group 1

Condition	Sample	Data	Mean hourly wind speed (m/s)
Normal wind conditions	Sample 1	Data 1	2.00
	Sample 2	Data 2	3.40
	Sample 3	Data 3	3.34
	Sample 4	Data 4	3.41
	Sample 5	Data 5	6.17
	Sample 6	Data 6	4.20
Typhoons	Maggie	Data 7	12.11
	Sam	Data 8	15.62
	York 1	Data 9	21.72
	York 2	Data 10	15.91

Table 2 Wind information for data in Group 2 with wind speeds of about 7.5 m/s

Condition	Data	Mean hourly wind speed (m/s)
Typhoons	Data 1	7.36
	Data 2	7.77
	Data 3	7.43

3. Bayesian method

The fast Bayesian FFT method is adopted in the present study to perform output-only modal identification. The algorithm is outlined as follows (Au and Zhang 2012, Au *et al.* 2013). For the detailed theory, please refer to Au (2011, 2012a, b) and Zhang and Au (2013).

The measured acceleration responses are assumed to be composed by the theoretical response and a prediction error

$$\hat{\ddot{\mathbf{x}}}_j = \ddot{\mathbf{x}}_j + \mathbf{e}_j \tag{1}$$

where $\ddot{\mathbf{x}}_j \in R^n$ and $\mathbf{e}_j \in R^n$ (j=1,2,…, N) denote the theoretical acceleration response and prediction error, respectively, with n being the number of measured degrees of freedom (DOFs) and N being the number of sampling points. The fast Fourier Transform (FFT) of $\hat{\ddot{\mathbf{x}}}_j$ is expressed by

$$F_k = \sqrt{\frac{2\Delta t}{N}} \sum_{j=1}^{N} \hat{\ddot{\mathbf{x}}}_j \exp[-2\pi \mathbf{i} \frac{(k-1)(j-1)}{N}] \tag{2}$$

where $\mathbf{i}^2 = -1$; Δt is the sampling interval; $k=1,\ldots, N_q$ with N_q =int[N/2]+1, N_q is the Nyquist frequency index; int [.] denotes the integer part.

Let $\mathbf{Z}_k = [\mathrm{Re}\, F_k; \mathrm{Im} F_k] \in R^{2n}$ represent a vector consisting of the real and imaginary parts of F_k. In this method, only the FFT data in a selected frequency band dominated by the target modes are used for modal identification, and they are denoted by $\{\mathbf{Z}_k\}$. Let $\boldsymbol{\theta}$ denote a vector of modal parameters to be identified. It includes modal frequencies, damping ratios, mode shapes, PSD matrix of the prediction error and PSD of modal force. Based on Bayes' Theorem, given the dataset, the conditional posterior probability density function (PDF) of $\boldsymbol{\theta}$ can be expressed by

$$p(\boldsymbol{\theta} | \{\mathbf{Z}_k\}) \propto p(\boldsymbol{\theta}) p(\{\mathbf{Z}_k\} | \boldsymbol{\theta}) \tag{3}$$

where $p(\boldsymbol{\theta})$ is the prior PDF of $\boldsymbol{\theta}$. For a large amount of data, the likelihood function varies fast compared to the prior PDF, and therefore it dominates the posterior PDF (Au *et al.* 2013). The prior information is assumed to be uniform, and then the posterior PDF $p(\boldsymbol{\theta} | \{\mathbf{Z}_k\})$ is proportional to the likelihood function $p(\{\mathbf{Z}_k\} | \boldsymbol{\theta})$. Thus, the most probable value (MPV) of $\boldsymbol{\theta}$ can be determined by maximizing $p(\{\mathbf{Z}_k\} | \boldsymbol{\theta})$.

Assuming large N and small Δt, the FFTs at different frequency bands are shown to be asymptotically independent and follow a Gaussian distribution (Schoukens and Pintelon 1991, Yuen and Katafygiotis 2003). Consequently, $p(\{\mathbf{Z}_k\}|\boldsymbol{\theta})$ can be expressed by

$$p(\{\mathbf{Z}_k\} | \boldsymbol{\theta}) = \prod_k (2\pi)^{-n} (\det \mathbf{C}_k)^{-1/2} \exp[-\frac{1}{2} \mathbf{Z}_k^T \mathbf{C}_k^{-1} \mathbf{Z}_k] \tag{4}$$

where $\det(.)$ denotes the determinant of its argument

$$\mathbf{C}_k = \frac{1}{2} \begin{bmatrix} \boldsymbol{\Phi} & \\ & \boldsymbol{\Phi} \end{bmatrix} \begin{bmatrix} \mathrm{Re}\, \mathbf{H}_k & -\mathrm{Im}\, \mathbf{H}_k \\ \mathrm{Im}\, \mathbf{H}_k & \mathrm{Re}\, \mathbf{H}_k \end{bmatrix} \begin{bmatrix} \boldsymbol{\Phi}^T & \\ & \boldsymbol{\Phi}^T \end{bmatrix} + \frac{S_e}{2} \mathbf{I}_{2n} \tag{5}$$

is the covariance matrix of $\mathbf{Z}_k$; $\boldsymbol{\Phi} = [\boldsymbol{\varphi}_1, \boldsymbol{\varphi}_2, ..., \boldsymbol{\varphi}_m] \in R^{n \times m}$ is the mode shape matrix with m being the number of modes in a selected frequency band; S_e is the PSD of the prediction error; $\mathbf{I}_{2n} \in R^{2n}$ is a $2n$ by $2n$ identity matrix; $\mathbf{H}_k \in R^{m \times m}$ is the transfer matrix and the (i, j) element of this matrix can be expressed as

$$\mathbf{H}_k(i, j) = S_{ij} [(\beta_{ik}^2 - 1) + 2\mathbf{i}\zeta_i \beta_{ik}]^{-1} [(\beta_{jk}^2 - 1) - 2\mathbf{i}\zeta_j \beta_{jk}]^{-1} \tag{6}$$

where the frequency ratio $\beta_{ik} = f_i / \mathrm{f}_k$; f_i is the ith modal frequency; f_k is the FFT frequency abscissa; ζ_i denotes the ith damping ratio; S_{ij} is the cross PSD between the ith and jth modal excitations. The negative log-likelihood function (NLLF) $L(\boldsymbol{\theta})$ is usually used to perform the

optimization

$$L(\boldsymbol{\theta}) = \frac{1}{2}\sum_{k}[\ln\det \mathbf{C}_k(\boldsymbol{\theta}) + \mathbf{Z}_k{}^T \mathbf{C}_k(\boldsymbol{\theta})^{-1}\mathbf{Z}_k] \tag{7}$$

so that

$$p(\boldsymbol{\theta}\,|\,\{\mathbf{Z}_k\}) \propto \exp[-L(\boldsymbol{\theta})] \tag{8}$$

Theoretically, the MPV of $\boldsymbol{\theta}$ including modal frequency, damping ratio, mode shape, PSD of the prediction error, PSD of modal force can be determined by minimizing the NLLF. It is found that, however, the minimization process is ill-conditioned and the computational amount grows with the number of measured DOFs. To make this method workable in practice, fast algorithms have been developed, allowing very quick calculation of the MPV (Au 2011, Au 2012a, b, Zhang and Au 2013). The associated posterior covariance matrix can also be determined as the inverse of the Hessian matrix, and it can be calculated analytically on the basis of the NLLF. This further makes it possible to quantitatively evaluate the posterior uncertainties of the modal parameters under identification.

4. Data analysis

4.1 Modal identification on the data of Group 1

Modal analysis is performed by the fast Bayesian FFT method on each data set. Figs. 2(a) and 2(b) show the time history of the acceleration responses from the first three channels for Sample 1 and Typhoon York 1, respectively. It was interesting to note that the responses from Chanel 1 and Chanel 3 in the vertical direction under normal wind conditions have larger magnitude than those under typhoon conditions.

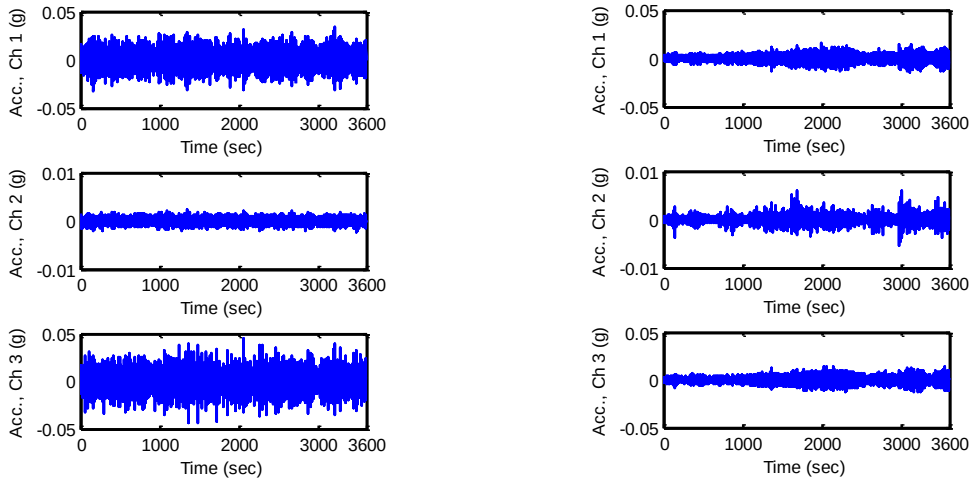

(a) Channels 1 to 3 for Sample 1

(b) Channels 1 to 3 for Typhoon York 1

Fig. 2 Accelerometer responses obtained from typical channels

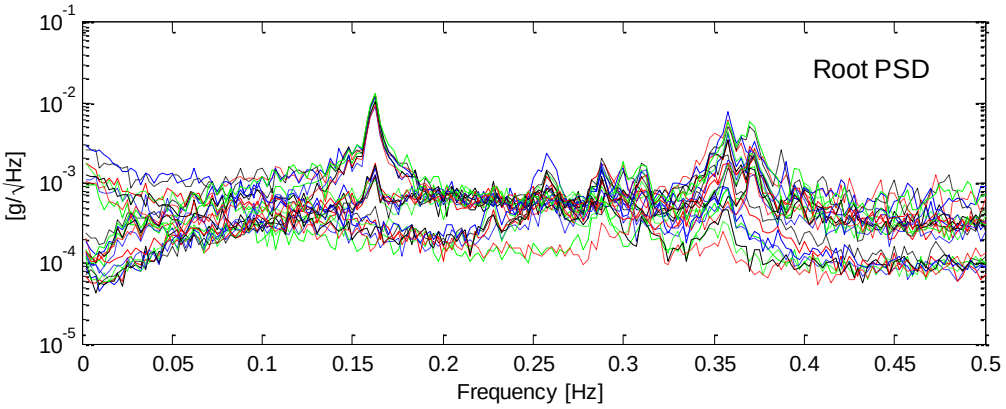

Fig. 3 Root power density spectra of response data in Sample 1

In contrast, the responses in the transverse direction under normal wind conditions are a little smaller than those obtained during typhoon events. This is because the bridge was closed without traffic operation during the typhoon attack. It turns out that the effect due to traffic loading is more significant than that due to strong wind in the vertical direction. In the transverse direction, however, the effect of typhoon is dominant.

To investigate the responses in the frequency domain, the root PSD spectra for the data in Sample 1 and Typhoon York 1 are obtained and plotted in Figs. 3 and 4, respectively. From the spectra, it is found that the first mode is about 0.16 Hz, and some peaks in Fig. 4 are more obvious than in Fig. 3 (such as the mode around 0.22 Hz). The modal responses for certain modes are much larger during the typhoons than during normal wind conditions.

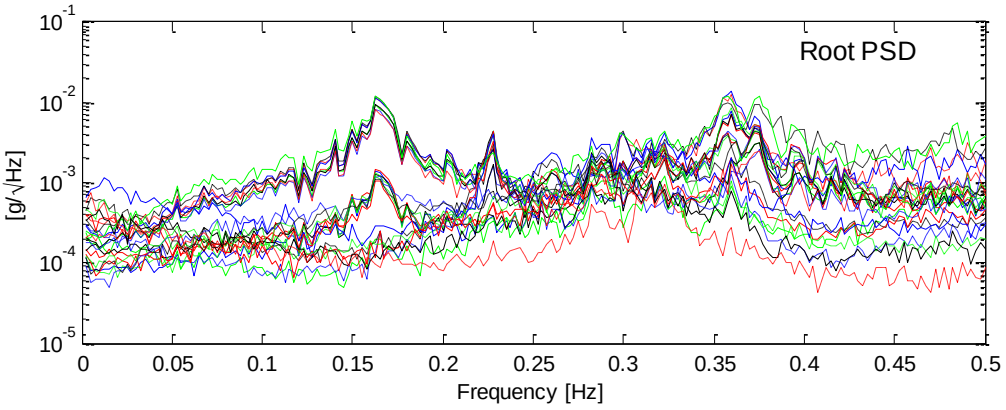

Fig. 4 Root power density spectra of response data in Typhoon York 1

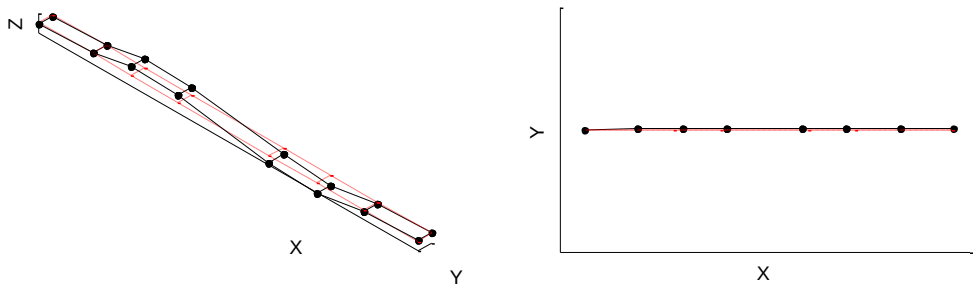

Fig. 5 Mode shape of the 1st mode from Sample 1 (0.161 Hz, 1.17%)

Fig. 5 to Fig. 14 show the modal parameters for ten modes identified using the data in Sample 1. In each figure, the left subfigure represents the motion in the vertical direction, while the right one represents the motion in the transverse direction. The first mode identified is a vertical mode with a modal frequency of 0.161 Hz and damping ratio of 1.17%. The mode shape in the vertical direction forms a sine wave. No obvious motion is observed in the transverse direction. The modal frequency and damping ratio of the second mode identified are 0.227 Hz and 0.73% respectively. This is a coupled torsional mode in the vertical direction and lateral mode in the transverse direction. It is seen that the motion in the vertical direction is a little strange. This may be attributed to the low s/n ratio as reflected in Fig. 3. The detailed reason will be discussed later. The third mode is a lateral mode with a modal frequency of 0.257 Hz and damping ratio of 1.32%. A sine wave is shown in the transverse direction. This is the second lateral mode of the bridge and there is almost no motion in the vertical direction. The fourth mode shown in Fig. 8 is the third lateral mode with a modal frequency of 0.288 Hz and damping ratio of 1.04%. Similar to the second mode, this mode is also coupled with torsional behavior. The motion in the transverse direction tends to be one and a half sine waves. Different from the second mode, the torsion mainly occurs at both sides of the deck section. The fifth mode shown in Fig. 9 is a predominantly vertical mode with a modal frequency of 0.300 Hz and damping ratio of 0.46%. The shape of this mode is similar to the first mode at the two sides of the deck section, but there is almost no motion at the four locations in the middle span. There is slight motion in the transverse direction. The sixth mode shown in Fig. 10 is the fourth lateral mode with a modal frequency of 0.310 Hz and damping ratio of 0.49%. This mode is also coupled with torsional behavior. The seventh to tenth are the modes mainly in the vertical direction, and with slight motion in the transverse direction. The modal parameters shown above are consistent with those obtained by a FEM analysis provided in Supplemental Document 1 of the benchmark problem and identified in a previous study by Ni *et al.* (2015a).

Figs. 15 and 16 show the posterior uncertainties of the identified modal frequencies and damping ratios for the first to fourth modes from the 10 data sets. The identified results from each data set are shown with a dot at the posterior MPV and an error bar covering two posterior standard deviations. It is seen that the posterior uncertainties of modal frequencies are much smaller than those of damping ratios, implying that the identification of the former quantity is more accurate. For the first, third and fourth modes (the second mode will be discussed later), the variation of the identified modal parameters is relatively small. The posterior uncertainty is consistent with the ensemble variability of their MPVs over different setups and therefore the

Bayesian and frequentist perspectives roughly agree. The error bars for the third and fourth modes from some data sets, such as the third mode from Data 5 and 9 and the fourth mode from Data 6 are larger than those from other data sets, but the variations are consistent for both modal frequency and damping ratio.

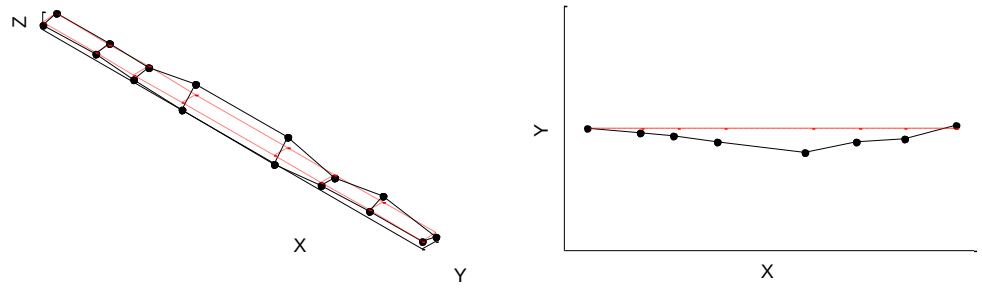

Fig. 6 Mode shape of the 2nd mode from Sample 1 (0.227 Hz, 0.73%)

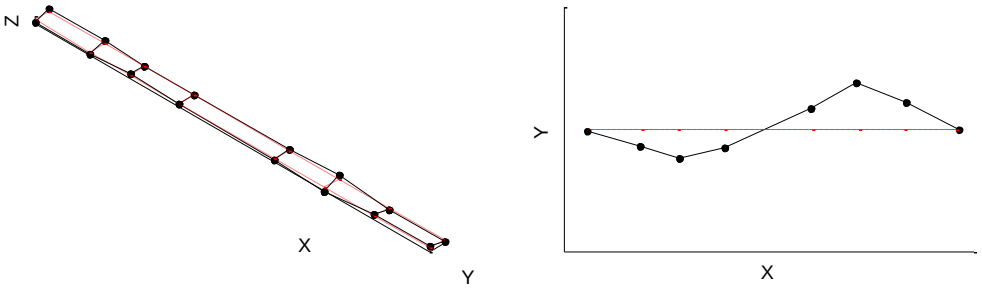

Fig. 7 Mode shape of the 3rd mode from Sample 1 (0.257 Hz, 1.32%)

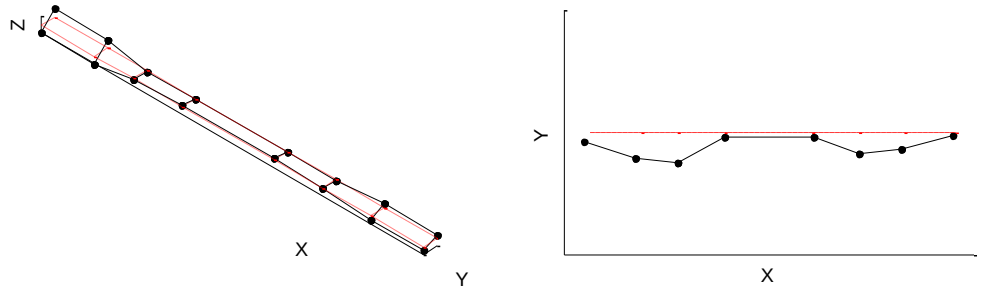

Fig. 8 Mode shape of the 4th mode from Sample 1 (0.288 Hz, 1.04%)

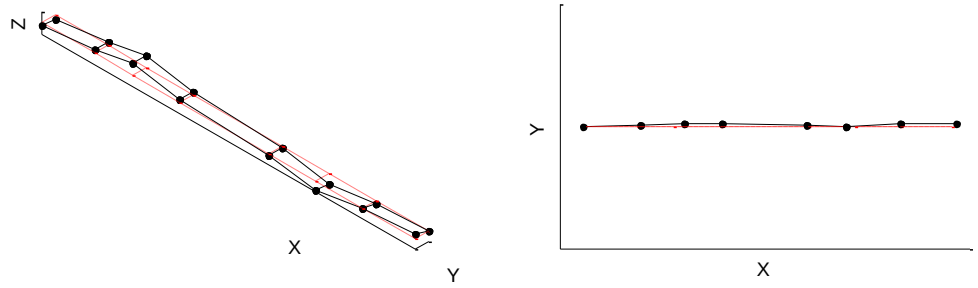

Fig. 9 Mode shape of the 5th mode from Sample 1 (0.300 Hz, 0.46%)

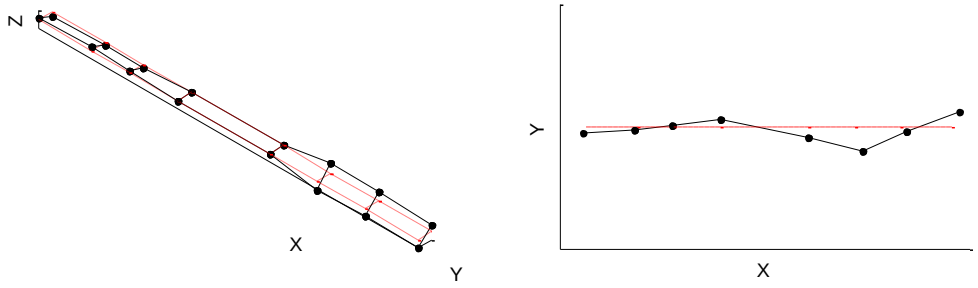

Fig. 10 Mode shape of the 6th mode from Sample 1 (0.310 Hz, 0.49%)

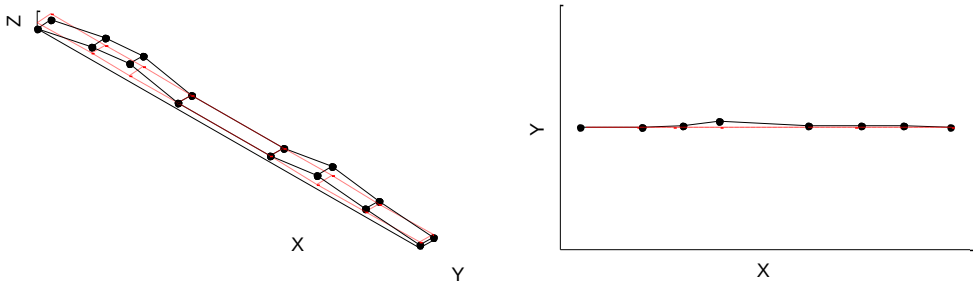

Fig. 11 Mode shape of the 7th mode from Sample 1 (0.357 Hz, 1.13%)

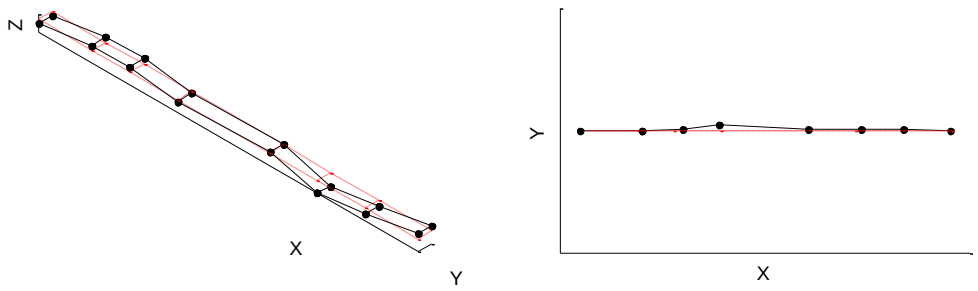

Fig. 12 Mode shape of the 8th mode from Sample 1 (0.372 Hz, 0.46%)

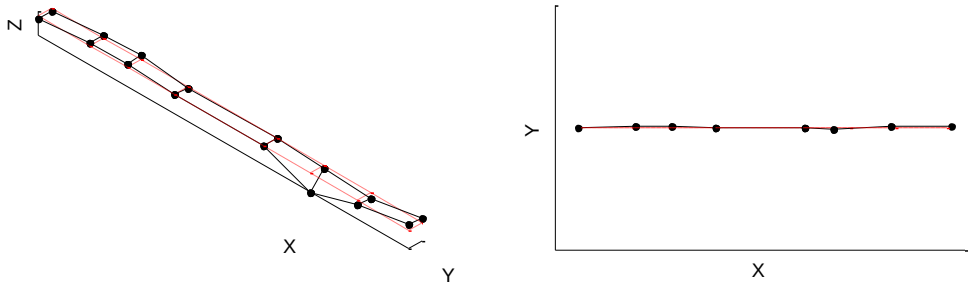

Fig. 13 Mode shape of the 9th mode from Sample 1 (0.385 Hz, 2.09%)

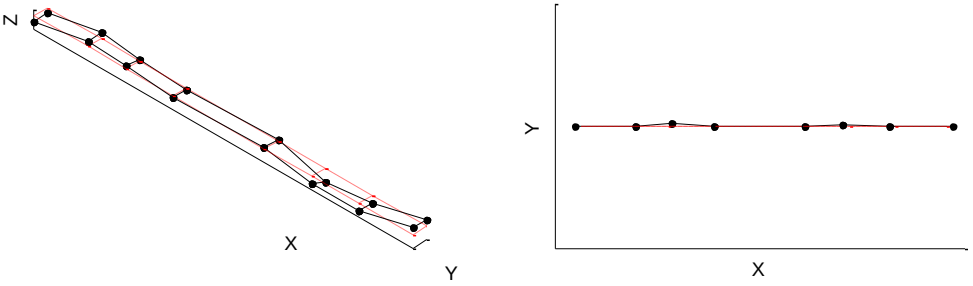

Fig. 14 Mode shape of the 10th mode from Sample 1 (0.396 Hz, 0.46%)

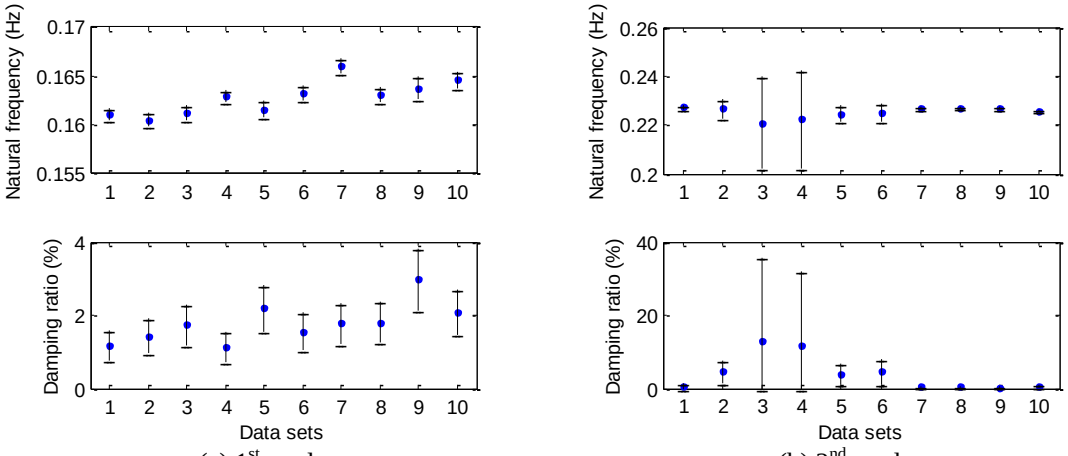

(a) 1st mode (b) 2nd mode

Fig. 15 Identification result (±2 standard derivation error bar) of modal frequency and damping ratio

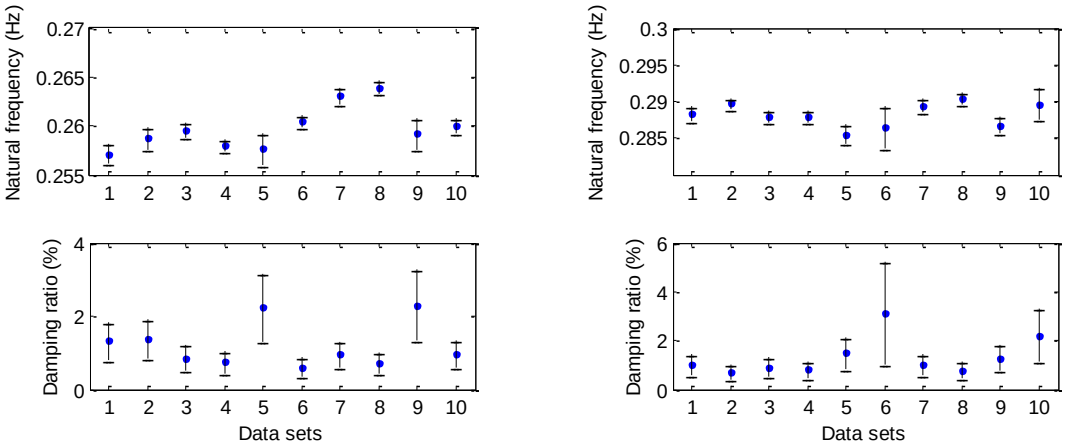

(a) 3rd mode (b) 4th mode

Fig. 16 Identification result (±2 standard derivation error bar) of modal frequency and damping ratio

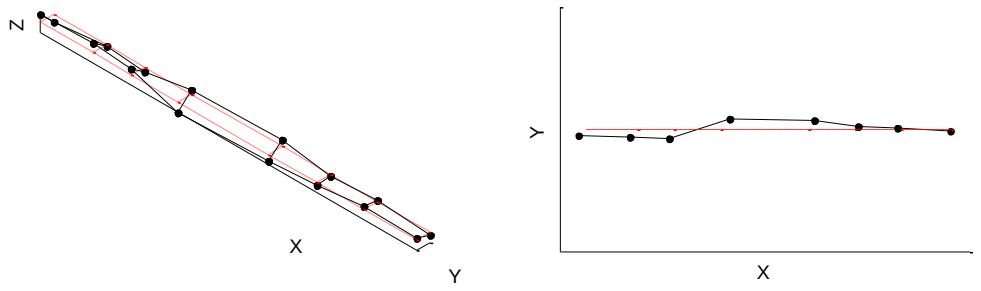

Fig. 17 Mode shape of the 2nd mode from Sample 2 (0.227 Hz, 4.56%)

It is worth mentioning that the second mode is quite different from the other three modes. The error bars corresponding to Data 2, 3, 4, 5 and 6 are obviously larger than those for other data sets, especially for the results from Data 3 and 4. The MPVs of modal frequencies are still acceptable; however, this is not the fact for the damping ratio with a value higher than 10%. Recall that these five data sets correspond to the samples under normal wind conditions. The considerably large error bars mean that under normal wind conditions, the identified modal parameters for this mode are not accurate or reliable. The posterior uncertainty of modal parameters obtained from Data 1 is reasonable, but the mode shape as shown in Fig. 6 is a little strange. Recall that from the PSD spectra, the second mode is not obvious under normal wind conditions. To make a further investigation, the mode shape identified from Sample 2 is obtained as shown in Fig. 17, where the motion in both vertical and transverse directions is different from that shown in Fig. 6. Similarly, the mode shapes of the second mode identified from Samples 3 to 6 are also different from each other. This indicates that the second mode might not be identifiable under normal wind conditions. In contrast, there is an obvious peak for the second mode in the PSD spectra obtained using the data from Typhoon York 1. Fig. 18 shows the mode shape of the second mode identified using the typhoon data. It is observed that the identified mode shape is more reasonable in terms of the modal motion in both directions.

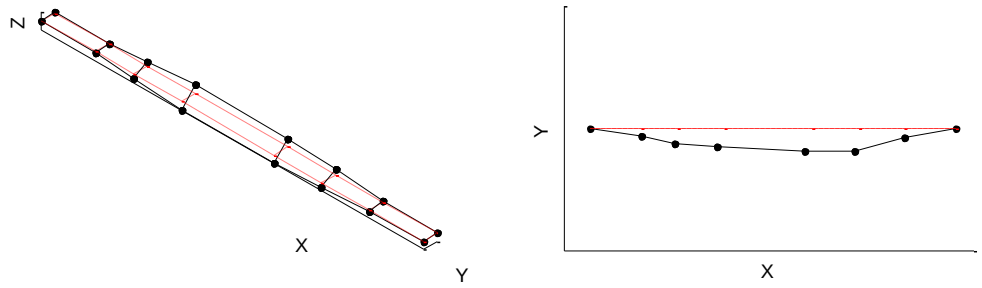

Fig. 18 Mode shape of the 2nd mode from Typhoon York 1 (0.227 Hz, 0.40%)

Table 3 MAC values between the mode shapes identified from data sets of Group 1 (2nd mode)

Mode 2	Data1	Data2	Data3	Data4	Data5	Data6	Data7	Data8	Data9	Data10
Data1	1.000	0.386	0.498	0.302	0.370	0.254	0.855	0.852	0.846	0.855
Data2	0.386	1.000	0.681	0.338	0.111	0.324	0.341	0.374	0.351	0.333
Data3	0.498	0.681	1.000	0.235	0.299	0.313	0.349	0.376	0.376	0.349
Data4	0.302	0.338	0.235	1.000	0.592	0.343	0.008	0.016	0.013	0.006
Data5	0.370	0.111	0.299	0.592	1.000	0.731	0.322	0.330	0.318	0.303
Data6	0.254	0.324	0.313	0.343	0.731	1.000	0.348	0.374	0.375	0.331
Data7	0.855	0.341	0.349	0.008	0.322	0.348	1.000	0.998	0.995	0.996
Data8	0.852	0.374	0.376	0.016	0.330	0.374	0.998	1.000	0.995	0.992
Data9	0.846	0.351	0.376	0.013	0.318	0.375	0.995	0.995	1.000	0.995
Data10	0.855	0.333	0.349	0.006	0.303	0.331	0.996	0.992	0.995	1.000

To compare the identified results from all the 10 data sets, the modal assurance criterion (MAC) among the mode shapes of the second mode identified respectively by the 10 data sets is calculated and shown in Table 3. It is seen that the MAC values among the results from the first six data sets are much less than 1, verifying the conclusion that the identified mode shapes are different from each other. For the results from the last four data sets, the MAC values among them are quite close to 1 (larger than 0.99), indicating that the identified mode shapes are identical. Note that the mode shapes of the second mode obtained by the data sets from Sample 1 and Typhoon York 1 are similar as shown in Figs. 6 and 18, with the MAC value between the mode shapes obtained by these two data sets being larger than 0.8. From the discussion above, it can be concluded that under normal wind conditions, the second mode is not identifiable. It can be well identified only when the wind speed reaches a certain value.

Table 4 Signal to noise ratios in different modes and data sets (Group 1)

Data \ Mode	1	2	3	4	5	6	7	8	9	10
1	1194	12	46	82	48	113	201	222	15	40
2	580	6	28	101	66	92	175	94	101	37
3	607	3	77	58	27	56	168	201	94	38
4	2689	3	145	111	73	77	314	456	66	77
5	696	4	23	47	45	45	365	194	21	50
6	698	4	135	15	34	53	488	167	19	49
7	1528	720	247	181	39	261	145	128	99	57
8	1150	603	306	102	44	124	465	87	34	84
9	1096	518	48	55	84	64	294	106	101	97
10	933	551	210	116	60	314	217	151	46	25

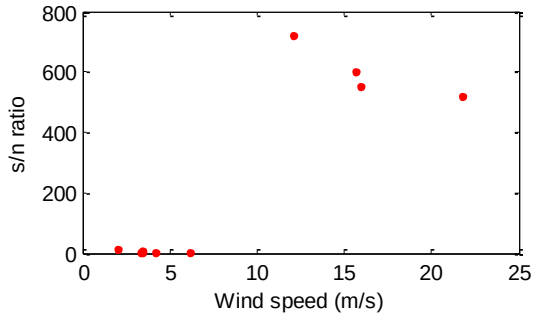

Fig. 19 Relationship between wind speed and s/n ratio for the 2nd mode

One explanation is that the s/n ratio for the second mode under normal wind conditions is too low. This issue will be discussed in detail in the following. In the fast Bayesian FFT method (Au 2011), the modal s/n ratio has been defined as follows

$$\gamma = \frac{S}{4S_e\zeta^2} \tag{9}$$

where S denotes the PSD of modal force; S_e denotes the PSD of the prediction error; and ζ denotes the damping ratio. Table 4 shows the s/n ratio calculated for different modes and from different data sets. It is seen that the s/n ratios obtained from the data acquired during typhoons tend to be larger than those obtained under normal wind conditions, especially for the second mode where a significant difference of the s/n ratio is observed among the data sets. The s/n ratio

values under the typhoon conditions are in the order of magnitude of a few hundred while they are less than or equal to 12 under normal wind conditions. This indicates that the s/n ratio is a useful quantity to evaluate the mode identifiability. If the s/n ratio is too small, the mode would not be identifiable. To further investigate this issue, the relationship between wind speed and s/n ratio is plotted in Fig. 19. It is observed that higher wind speed corresponds to larger s/n ratio. Based on these results, currently it is difficult to give an exact s/n ratio to judge the mode identifiability. Since the majority of the s/n ratio values corresponding to the identifiable cases in Table 4 are larger than 50, it is suggested to roughly take 50 as the bottom line to judge whether or not a mode is identifiable.

4.2 Modal identification on the data of Group 2

The three data sets of Group 2 are used to perform further investigation. One common feature of these data is that the corresponding wind speeds are all around 7.5 m/s. This is a critical value given in a previous study by Ni *et al*. (2015a) to examine whether the second mode is identifiable. The Fast Bayesian FFT method is applied again to these data sets. Table 5 shows the MAC values between the identified mode shapes of the second mode from the three data sets. It is seen that the MAC values between Data 2 and Data 3 are quite close to 1, while this is not the fact for those between Data 1 and Data 2 and between Data 1 and Data 3. Table 6 shows the s/n ratio calculated based on the identified modal parameters. The values of the s/n ratio for the second mode obtained from the three data sets are all larger than the critical value of 50 suggested in the previous section, although the value from Data 1 is only 77. As a result, the second mode shall be identifiable from all the three data sets. To confirm this, the mode shapes of the second mode identified from the first two data sets are plotted in Figs. 20 and 21, respectively. It is seen that the second mode is just marginally identifiable from Data 1, with the motion in the vertical direction being similar to that from Data 2; however, the motion in the transverse direction identified by the two data sets is different from each other.

Table 5 MAC values between the mode shapes identified from data sets of Group 2 (2^{nd} mode)

Mode 2	Data1	Data2	Data3
Data1	1.000	0.572	0.578
Data2	0.572	1.000	0.995
Data3	0.578	0.995	1.000

Table 6 Signal to noise ratios in different modes and data sets (Group 2)

Data \ Mode	1	2	3	4	5	6	7	8	9	10
1	1581	77	6	48	124	106	943	153	46	45
2	2491	191	654	90	57	255	406	110	51	76
3	1232	1154	830	997	26	847	130	38	38	31

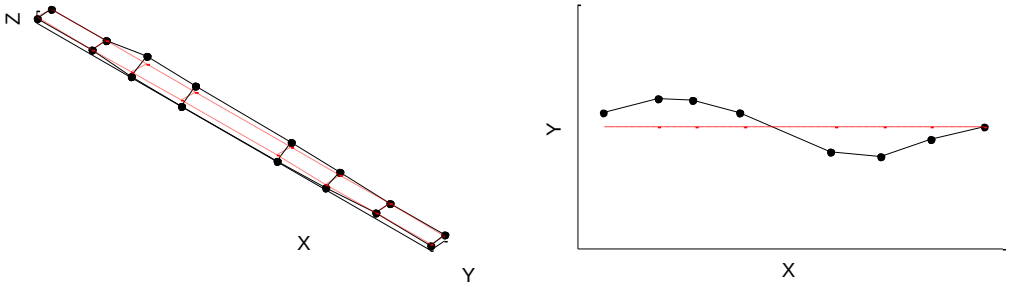

Fig. 20 Mode shape of the 2nd mode from Data 1 of Group 2 (0.229 Hz, 1.25%)

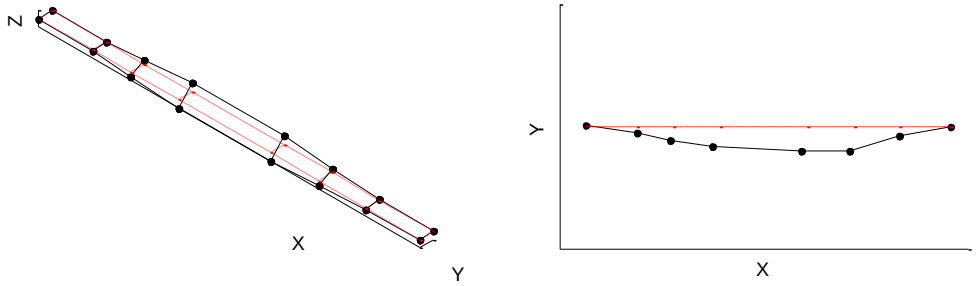

Fig. 21 Mode shape of the 2nd mode from Data 2 of Group 2 (0.228 Hz, 1.13%)

4.3 Modal identification on the data of Group 3

In this benchmark study, six blind data sets are also used to verify the conclusions obtained in the above sections. The blind data are provided without knowledge about the wind condition. Table 7 shows the MAC values between the identified mode shapes of the second mode from the six blind data sets. It is seen that the values from the first four data sets are larger than 0.6, especially for Data 1, 2 and 4 whose MAC values are quite close to 1 (larger than 0.98). By plotting the mode shapes identified using these three data sets, it is found that they are all consistent and reasonable. The mode shape obtained from Data 3 is also obtained and shown in Fig. 22. In this figure, the motion in the vertical direction is agreeable while the one in the transverse direction is not. This means that the mode is marginally identifiable. Table 8 shows the s/n ratio obtained from the six blind data sets. The values for the second mode from Data 1 and 2 are larger than 1,000, indicating that the mode is reliably identifiable from these two data sets. For Data 3, the value is equal to 28, which is slightly less than the critical value. It is found that only the mode shape in the vertical direction is identifiable from this data set. For Data 4, the value is marginally larger than the critical value, but the mode shape is identifiable as expected. Data 5 and 6 give rise to very low s/n ratio for the second mode; they are unable to provide correct identification of the mode shape.

Table 7 MAC values between the mode shapes identified from data sets of Group 3 (2nd mode)

Mode 2	Data 1	Data 2	Data 3	Data 4	Data 5	Data 6
Data 1	1.000	1.000	-0.635	0.988	-0.145	-0.127
Data 2	1.000	1.000	-0.625	0.989	-0.154	-0.143
Data 3	-0.635	-0.625	1.000	-0.643	0.105	0.022
Data 4	0.988	0.989	-0.643	1.000	-0.180	-0.214
Data 5	-0.145	-0.154	0.105	-0.180	1.000	0.343
Data 6	-0.127	-0.143	0.022	-0.214	0.343	1.000

Table 8 Signal to noise ratios in different modes and data sets (Group 3)

Data \ Mode	1	2	3	4	5	6
1	9873	5966	957	1076	164	777
2	6169	2441	1063	390	49	865
3	1315	28	13	47	93	57
4	679	92	255	69	24	128
5	1788	3	122	119	46	87
6	938	4	28	32	27	115

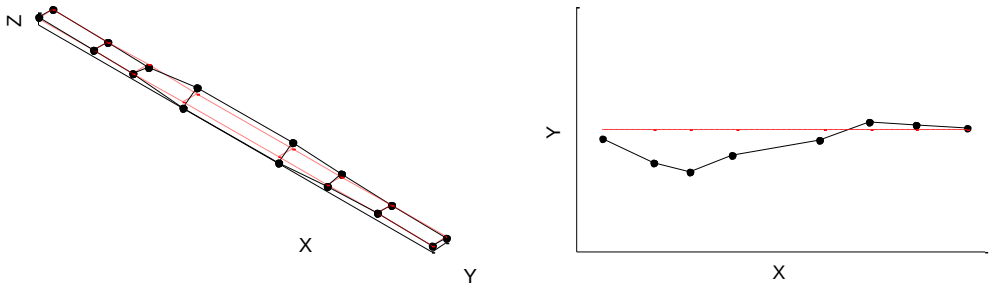

Fig. 22 Mode shape of the 2nd mode from Data 3 of Group 3 (0.225 Hz, 2.16%)

5. Conclusions

The mode identifiability of a cable-stayed bridge using ambient vibration data has been studied by the fast Bayesian FFT method. The acceleration response data acquired from the bridge under normal wind conditions and under typhoon conditions are used for this study. It is found that the

second mode is a deficient mode which cannot be reliably identified when using the data acquired under normal wind conditions. With the identified most probable values (MPVs) and the associated posterior uncertainties of modal parameters from the fast Bayesian FFT method, the signal to noise (s/n) ratio values are derived to evaluate the mode identifiability of target modes. Based on the modal analysis results from thirteen non-blind data sets, a critical value equal to about 50 is suggested for the s/n ratio to examine the mode identifiability of the second mode given measured acceleration data from the bridge.

The modal s/n ratio and its critical value have been verified using six blind data sets without knowledge about the wind condition. It is found that the first two data sets lead to very high values of the s/n ratio (much higher than the critical value) for the second mode, indicating the capability of reliably identifying the mode shape from these two data sets. The third and fourth data sets generate the s/n ratio values for the second mode close to the critical value: one is slightly less than the critical value and the other is slightly larger than the critical value. As a result, it is marginal to identify the second mode by using these two data sets. Because of giving rise to very low values of the s/n ratio (much lower than the critical value) for the second mode, the fifth and sixth data sets are definitely unable to correctly identify the mode shape of the second mode. The above conclusions have been confirmed by comparing the identified mode shapes from the blind data with those from the non-blind data acquired under typhoon conditions.

Acknowledgements

This paper is funded by Natural Nature Science Foundation of China (Grant Nos.: 51508407, 51508413), Shanghai Pujiang Program (Grant No.: 15PJ1408600), MOR-NSFC Joint Research Program (Project No. U1234210) and the Grant from the Fundamental Research Funds for the Central Universities, China (Grant No. 2014KJ040). The financial support is gratefully acknowledged.

References

Au, S.K. (2011). "Fast Bayesian FFT method for ambient modal identification with separated modes", *J. Eng. Mech. - ASCE*, **137**, 214-226.

Au, S.K. (2012a), "Fast Bayesian ambient modal identification in the frequency domain, Part I: Posterior most probable value", *Mech. Syst. Signal Pr.*, **26**, 60-75.

Au, S.K. (2012b), "Fast Bayesian ambient modal identification in the frequency domain, Part II: posterior uncertainty", *Mech. Syst. Signal Pr.*, **26**, 76-90.

Au, S.K., Ni, Y.C., Zhang, F.L. and Lam, H.F. (2012a), "Full scale dynamic testing of a coupled slab system", *Eng. Struct.*, **37**, 167-178.

Au, S.K. and Zhang, F.L. (2012a), "Fast Bayesian ambient modal identification incorporating multiple setups", *J. Eng. Mech. - ASCE*, **138**(7), 800-815.

Au, S.K. and Zhang, F.L. (2012b), "Ambient modal identification of a primary-secondary structure by Fast Bayesian FFT method", *Mech. Syst. Signal Pr.*, **28**, 280-296.

Au, S.K., Zhang, F.L. and Ni, Y.C. (2013), "Bayesian operational modal analysis: theory, computation, practice", *Comput. Struct.*, **126**, 3-15.

Au, S.K., Zhang, F.L. and To, P. (2012b), "Field observations on modal properties of two tall buildings under strong wind", *J. Wind Eng. Ind. Aerod.*, **101**, 12-23.

Bao, Y., Beck, J.L. and Li, H. (2011), "Compressive sampling for accelerometer signals in structural health monitoring", *Struct. Health Monit.*, **10**(3), 235-246

Brincker, R., Zhang, L. and Anderson, P. (2001), "Modal identification of output-only systems using frequency domain decomposition", *Smart Mater. Struct.*, **10**, 441-455.

Brownjohn, J.M.W., Magalhaes, F., Caetano, E. and Cunha, A. (2010), "Ambient vibration re-testing and operational modal analysis of the Humber Bridge", *Eng. Struct.*, **32**(8), 2003-2018.

Brownjohn, J.M.W., Moyo, P., Omenzetter, P. and Chakraborty, S. (2005), "Lessons from monitoring the performance of highway bridge", *Struct. Control Health Monit.*, **12**, 227-244.

Cross, E.J., Koo, K.Y., Brownjohn, J.M.W. and Worden, K. (2013), "Long-term monitoring and data analysis of the Tamar Bridge", *Mech. Syst. Signal Pr.*, **35**, 16-34.

Ko, J.M. and Ni, Y.Q. (2005), "Technology developments in structural health monitoring of large-scale bridges", *Eng. Struct.*, **27**(12), 1715-1725.

Koo, K.Y., Brownjohn, J.M.W., List, D.I. and Cole, R. (2013), "Structural health monitoring of the Tamar suspension bridge", *Struct. Control Health Monit.*, **20**(4), 609-625.

Lam, H.F., Peng, H.Y. and Au, S.K. (2014), "Development of a practical algorithm for Bayesian model updating of a coupled slab system utilizing field test data", *Eng. Struct.*, **79**, 182-194.

Li, H., Ou, J., Zhao, X., Zhou, W., Li, H., Zhou, Z. and Yang, Y. (2006), "Structural health monitoring system for the Shandong Binzhou Yellow River highway bridge", *Comput.- Aided Civil Infrastructu. Eng.*, **21**(4), 306-317.

Ni, Y.C. and Au, S.K. (2014), "Fast Bayesian modal identification of structures using known single-input forced vibration data", *Struct. Control Health Monit.*, **21**(3), 381-402.

Ni, Y.C., Lu, X.L. and Lu, W.S. (2016). "Field dynamic test and Bayesian modal identification of a special structure – the Palms Together Dagoba", *Struct. Control Health Monit.*, In press. DOI: 10.1002/stc.1816.

Ni, Y.Q., Wang, Y.W. and Xia, Y.X. (2015a), "Investigation of mode identifiability of a cable-stayed bridge: comparison from ambient vibration responses and from typhoon-induced dynamic responses", *Smart Struct. Syst.*, **15**(2), 447-468.

Ni, Y.Q., Wong, K.Y. and Xia, Y. (2011), "Health checks through landmark bridges to sky-high structures", *Adv. Struct. Eng.*, **14**(1), 103-119.

Ni, Y.Q., Zhang, F.L., Xia, Y.X. and Au, S.K. (2015b), "Operational modal analysis of a long-span suspension bridge under different earthquake events", *Earthq. Struct.*, **8**(4), 859-887.

Peeters, B. and De Roeck, G. (2001), "Stochastic system identification for operational modal analysis: a review", *J. Dynam. Syst. Measurement Control - ASME*, **123**(4), 659-667.

Schoukens, J. and Pintelon, R. (1991), *Identification of Linear Systems: A Practical Guideline for Accurate Modelling*, London: Pergamon Press.

Yuen, K.V. and Katafygiotis, L.S. (2003), "Bayesian fast fourier transform approach for modal updating using ambient data", *Adv. Struct. Eng.*, **6**(2), 81-95.

Zhang, F.L. and Au, S.K. (2013), "Erratum for Fast Bayesian FFT method for ambient modal identification with separated modes by Siu-Kui Au", *J. Eng. Mech. - ASCE*, **139**, 545-545.

Zhang, F.L., Au, S.K. and Lam, H.F. (2015), "Assessing uncertainty in operational modal analysis incorporating multiple setups using a Bayesian approach", *Struct. Control Health Monit.*, **22**, 395-416.

Zhang, F.L., Ni, Y.Q., Ni, Y.C. and Wang, Y.W. (2016), "Operational modal analysis of Canton Tower by a fast frequency domain Bayesian method", *Smart Struct. Syst.*, **17**(2), 209-230.